Hindawi
Shock and Vibration
Volume 2020, Article ID 6717128, 12 pages
https://doi.org/10.1155/2020/6717128

Research Article

Identification of Microseismic Signals Based on Multiscale Singular Spectrum Entropy

Xingli Zhang, Zhenhua Zhao, Ruisheng Jia, and Lianyue Cao

College of Computer Science and Engineering, Shandong University of Science and Technology, Qingdao 266590, China

Correspondence should be addressed to Xingli Zhang; xlzhang_only@163.com

Received 17 December 2019; Revised 8 May 2020; Accepted 12 May 2020; Published 28 May 2020

Academic Editor: Roberto Palma

The accurate identification of effective microseismic events has great significance in the monitoring, early warning, and forecasting of rockburst hazards. However, the conventional identification methods have displayed difficulties in achieving satisfactory results. A microseismic signal identification method which combines variational mode decomposition (VMD) and multiscale singular spectrum entropy was proposed in this paper. The original signal was firstly broken down into a given number K variational mode components, which are ranked by frequency in descending order. Then, the characteristic pattern matrix was constructed according to the mode component signals, and the identification model of the microseismic signals based on the support vector machine was built by performing a multiscale singular spectrum entropy calculation of the collected vibration signals, constructing eigenvectors of signals. Finally, a comparative analysis of the microseismic events and blasting vibration signals in the experiment proved that the different characteristics of the two kinds of signals can be fully expressed by using multiscale singular spectrum entropy. Experimental results further confirmed the effective identification performance of this proposed method.

1. Introduction

In recent years, microseismic monitoring has become an advanced and effective means for monitoring rock and coal dynamical disasters. It can be carried out in real time for the continuous and online monitoring of the microseismic activities of rock fractures and thereby has become a useful source of microseismic monitoring data. It is well known that the mining environment is very complex due to the large amounts of noise signals such as the background noise and blasting vibrations. These noise signals generally cause the inaccurate identification of the microseismic signals in microseismic monitoring systems. In addition, technical personnel are required to manually identify effective microseismic events, which seriously affect the efficiency of the microseismic monitoring systems. Considering the fact that blasting operations often occur in coal mines, and the waveforms of rock fractures and blasting vibrations are very similar, the artificial identification method often makes processing errors, which is difficult to effectively identify.

Presently, the identification methods used for the microseismic signal mainly include the first arrival times of the seismic phases, feature recognitions, and parameter discriminations. The most commonly used seismic phase first arrival methods include a STA/LTA (short-time average/long-time average) method and AIC (Akaike information criterion) criterion. The STA/LTA method [1–3] dynamically reflects the amplitude changes of the signals using the energy average of the short-term window of the time domain, along with the energy average of the long-term window. This method is able to automatically detect microseismic events by identifying their first arrival times. The STA/LTA method is known to be simple and fast. However, the error rates have been considered to be slightly high, especially when the signal-to-noise ratio is low. Also, the automatic detection function of the method has been found to be unreliable, and the antinoise performances of the algorithm have been observed to be poor. The AIC method was proposed to distinguish the first arrivals of the seismic phases based on the statistical

differences in the wave data before and after the arrivals of seismic waves [4]. It has been observed that the AIC function is sharp in the local minimum peak at the beginning of earthquake phases, and the minimum points of the AIC values are the demarcation points of two stable time series. However, due to the fact that the actual microseismic signals are nonstationary signals, the identification effects of the AIC method tend to be greatly influenced by the window selections and signal-to-noise ratios. The feature recognition method mainly uses Fourier transform, wavelet transform, empirical mode decomposition (EMD), and other time-frequency analysis methods to extract signal features and identify signals. Lu et al. [5] used the Fourier transform to analyze the power spectrum and amplitude frequency characteristics of roof-pressure relief-blasting microseismic signals and coal-seam pressure-blasting microseismic signals and preliminarily identified the different types of microseismic signals in mines. However, the Fourier transform is traditionally used to analyze periodic stationary signals and has not been found to be effective for random nonstationary microseismic signals with spikes and mutations [6, 7]. Wavelet analysis can simultaneously perform time and frequency analyses [8]. However, this type of analysis requires the choosing of a suitable wavelet base to achieve better decomposition effects [9, 10]. Presently, many researchers have applied wavelet analysis to the waveform characteristics of natural earthquakes [11, 12] and energy variation of seismomagnetic signals [13], as well as the analyses of microseismic signals in mines [14], and so on, and have achieved better application results. Empirical mode decomposition, which was proposed by Huang et al. [15], is an algorithmic method used to detect and decompose a signal into principal "modes." This method has been proven to be suitable for handling random nonstationary signals. Scholars have applied it to the noise reduction of mine microseismic signals [16], feature extraction [17], classification identification [18, 19], and other fields. However, there have been boundary effects and a mode-aliasing phenomenon observed in the EMD method [20, 21], which causes the decomposition results to experience problems, such as instability and nonuniqueness. These defects in the EMD make it difficult to effectively identify signals. As a novel method for signal identification, the combination of deep learning technology and feature extraction has attracted the interest of many researchers [22, 23]. The parameter discrimination used a linear regression fitting method [24, 25] and extracted the two slope values of the starting-up trend line and the two coordinate values of the first and maximum peaks as the characteristic parameters. Then, it established an identification model by applying a Fisher discriminant analysis [26]. However, this method required a higher signal waveform, which also resulted in difficulties in the identification of signals.

Variational mode decomposition (VMD) is an entirely nonrecursive decomposition model in which the band-limited intrinsic mode functions (BLIMFs) or modes are extracted concurrently [27]. The model searches for mode ensembles, as well as their respective center frequencies, in which the modes collectively reproduce the input signals, while each becomes smooth after demodulation into a baseband. The VMD method has a strong theoretical foundation which overcomes the shortcomings of the boundary effects and mode-aliasing phenomenon of the EMD and other recursive decomposition algorithms. Also, the VMD method avoids the difficulties of selecting the wavelet base functions of wavelet or wavelet packet analyses. At the present time, the VMD method has been successfully applied to the functional coupling analyses of electroencephalograms and electromyograms [28], fault diagnoses [29], and feature extractions [30, 31], as well as other fields. Singular spectrum entropy has been widely used to analyze a signal's sequence complexity analysis and perform nonlinearity analysis because of its high robustness and antinoise. Multiscale singular spectrum entropy (MSSE) is a combination of multiscale and singular spectrum entropy and is more effective for analyzing the information of a time sequence. It has been applied to the isolated island detection in power grids [32], fault diagnoses [33–35], and other fields. The support vector machine is based on a statistical theory that follows the principle of structural risk minimization and considers the empirical risk as well as the confidence risk. In a small sample, nonlinear and high-dimensional pattern recognition problems are used and show many unique advantages [36]. In the case of wired data samples, the data sample features can be well described and have been widely used in fault diagnosis, pattern recognition, and other fields [37, 38]. The least-squares support-vector machine (LS-SVM) is based on the regularization theory [39], which solves the quadratic programming problem in the classical SVM algorithm to solve linear equations, improves the convergence speed of the algorithm, and reduces the time needed to perform the algorithm. The above analysis shows that MSSE can reflect the essential characteristics of a one-dimensional time series from different aspects, is sensitive to the complexity of signals at different scales, and can fully express the different characteristics of microseismic signals and blasting vibration signals. A LS-SVM classifier can be trained by learning microseismic signal samples and blasting vibration signal samples. A LS-SVM classifier can accurately identify microseismic signals, so this paper introduces multiscale singular spectrum entropy to measure microseismic signal complexity, and the LS-SVM model was used to identify microseismic events.

In view of the shortcomings of the abovementioned multiscale decomposition methods and the limitations of feature extraction methods, in this paper a combination of MSSE and SVM, named MSSE-SVM, is proposed to identify microseismic signals. The signal is firstly broken down into the K modes through VMD, and then the singular spectrum entropy of each mode is estimated using MSSE; finally, the singular spectrum entropy eigenvector is input into the trained classifier to identify the signal type. In order to verify the identifying effectiveness, this proposed MSSE-SVM method is applied to a large number of historical sample data. Compared to EMD-based techniques and energy characteristic methods, The MSSE characteristic can distinguish microseismic signals from blasting vibration signals, and has better accuracy and stability.

2. Theoretical Background

2.1. Variational Mode Decomposition. The VMD algorithm is a new completely nonrecursive signal decomposition method [27], it can adaptively decompose any signal x into the K discrete number of the subsignals (modes) $u_k\,(k = 1, 2, \ldots, K)$, where each mode is a limited bandwidth and compact around their respective center frequencies $\omega_k\,(k = 1, 2, \ldots, K)$. The constraint condition is that the sum of the bandwidth of all modes is the smallest, and the sum of all the modes is equal to the input signal x. The VMD algorithm suggests to making use of both a quadratic penalty term α and Lagrangian multipliers λ to address the constrained problem, in order to render the problem unconstrained. An alternate direction method of multipliers algorithm was used to obtain the optimal solution of the constrained variational problem, and the input signal is decomposed into each mode and its central frequency adaptively.

The concrete steps of VMD were as follows:

Input: the original signal x and the decomposition number K.

Output: K modes.

Step 1: initialize each mode $\{\widehat{u}_k^1\}$, central frequency $\{\widehat{\omega}_k^1\}$, and Lagrangian multipliers $\widehat{\lambda}^1$, and $n = 0$ and $\alpha = 2000$.

Step 2: $n = n + 1$, and update u_k and ω_k according to the following equations:

$$\widehat{u}_k^{n+1}(\omega) = \frac{\widehat{x}(\omega) - \sum_{i<k}\widehat{u}_i^{n+1}(\omega) - \sum_{i>k}\widehat{u}_i^{n}(\omega) + \left(\widehat{\lambda}^n(\omega)/2\right)}{1 + 2\alpha\left(\omega - \omega_k^n\right)^2}, \tag{1}$$

$$\omega_k^{n+1} = \frac{\int_0^\infty \omega\left|\widehat{u}_k^{n+1}(\omega)\right|^2 \mathrm{d}\omega}{\int_0^\infty \left|\widehat{u}_k^{n+1}(\omega)\right|^2 \mathrm{d}\omega}. \tag{2}$$

Step 3: update λ according to the following equation:

$$\widehat{\lambda}^{n+1}(\omega) = \widehat{\lambda}^n(\omega) + \tau\left(\widehat{x}(\omega) - \sum_k \widehat{u}_k^{n+1}(\omega)\right), \tag{3}$$

where τ represents the update step parameter of the Lagrangian multiplier.

Step 4: for a given discriminant accuracy $\varepsilon > 0$, if equation (4) is satisfied, then stop the iteration and output the K modes; otherwise, go back to Step 2:

$$\sum_k \frac{\left\|\widehat{u}_k^{n+1} - \widehat{u}_k^n\right\|_2^2}{\left\|\widehat{u}_k^n\right\|_2^2} < \varepsilon, \tag{4}$$

where ε is the convergence tolerance level, which can control the relative error effectively. In VMD algorithm, the default value of ε is $1e-6$. In this paper, the value of ε is $1e-7$.

Figure 1 depicts as an example of the decomposition of the noisy triharmonic signal with length 1000. It is affected by noise:

$$f_n(t) = \cos(4\pi t) + \frac{1}{4}\cos(48\pi t) + \frac{1}{16}\cos(576\pi t) + \eta, \tag{5}$$

where $\eta \sim N(0, 0.1)$ represents the Gaussian additive noise. Figure 1(b) shows the five IMFs from EMD. Figure 1(c) shows the BLIMFs extracted by VMD, where the number K is set to 5 to coincide with EMD.

As shown in Figure 1, the EMD produces 5 estimated modes. The first IMF contains the highest-frequency harmonic and amounts of noise but is severely distorted. The last two IMFs contain the middle and the lowest-frequency harmonics; however, serious mode aliasing has been appeared in these two IMFs. In the 5 BLIMFs extracted by VMD, the first two modes perfectly extracted the lowest-frequency and the middle harmonics. The forth mode contains the highest-frequency harmonic and small amount of noise. Figures 1(d) and 1(e) show that the frequency of BLIMFs is more compact and clear than that of IMFS. These demonstrate that the VMD decomposition performance is better than EMD.

In general, VMD is a powerful signal decomposition method. It has a solid foundation of mathematical theory and can solve the mode-aliasing problem better. Its operation is carried out in the frequency domain, and the operation efficiency is high. This paper uses these advantages of the VMD method to decompose the two kinds of vibration signals, so as to achieve the purpose of accurate calculation of the signal frequency band singular spectrum entropy and the extraction of multiscale singular spectrum entropy eigenvectors.

2.2. Multiscale Singular Spectrum Entropy. Singular spectrum analysis is an effective time-domain analysis method. It transforms the embedded space into an equivalent orthogonal coordinate system and obtains the signal trajectory in the subspace with the minimum embedding dimension. It eliminates the linear dependence and artificial symmetry between the delay coordinates, enhances the signal-to-noise ratio, and sharpens the singularity of the signal. However, as a time domain analysis method, traditional singular spectrum analysis is not conducive to multiscale monitoring and feature extraction of signal singularity. On this basis, a novel microseismic identification method that combines multiscale analysis and singular spectral entropy is proposed in this paper. By calculating the singular spectrum entropy of the components in different frequency bands, the uncertainty of the distribution of a singular characteristic in the different frequency space of the analyzed signal is accurately reflected.

Given the one-dimensional time series $x = \{x_1, x_2, \ldots, x_N\}$, the number of the total sampling points was represented as N, x was decomposed using the VMD method, and the K modes were denoted as

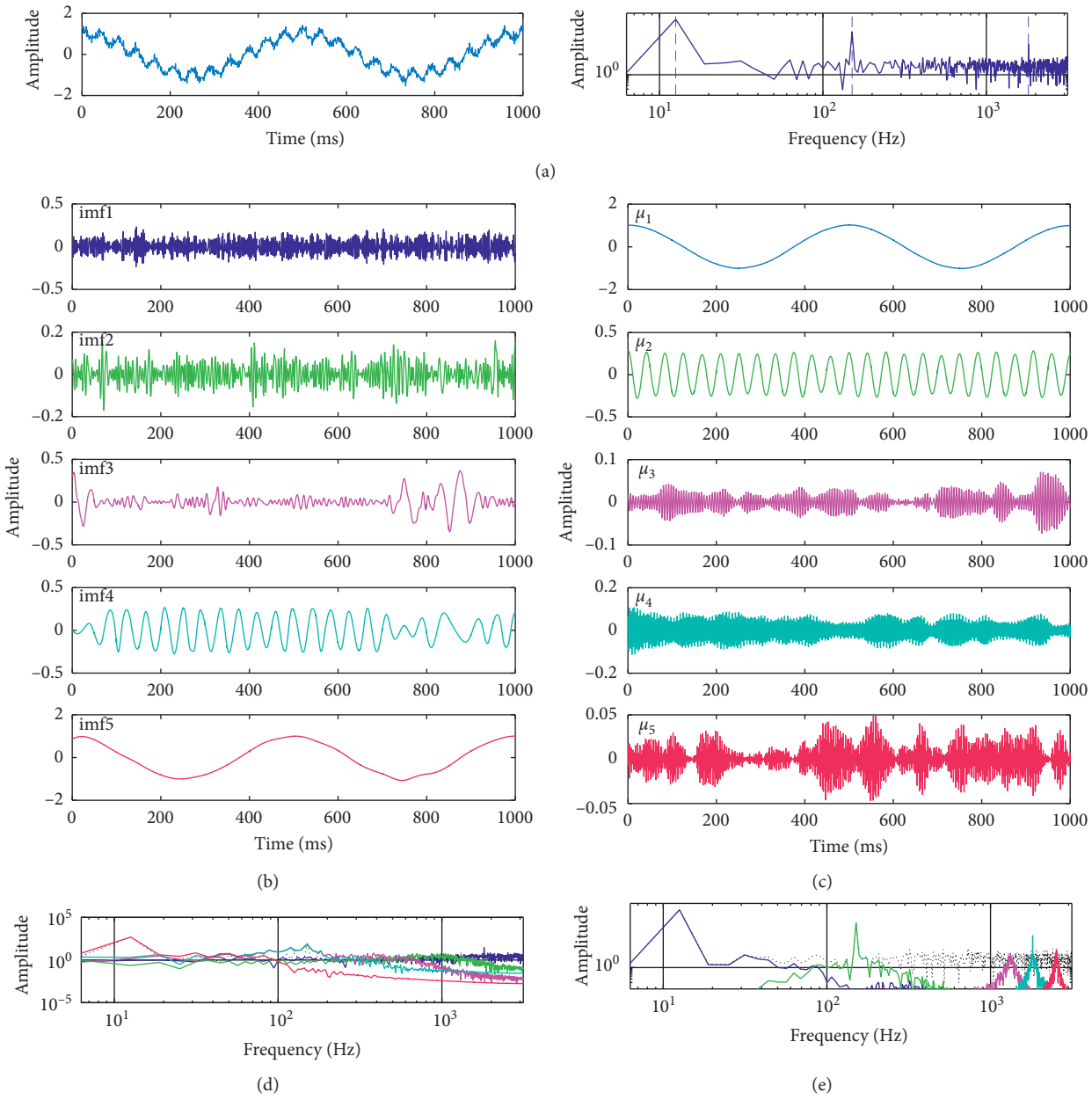

Figure 1: Decomposition of noisy triharmonic signal by EMD and VMD. (a) Noisy triharmonic signal and its spectrum. (b) EMD of noisy triharmonic signal with its IMF1-5. (c) VMD of noisy triharmonic signal with its u_1–u_5. (d) Decomposed spectral by EMD. (e) Decomposed spectral by VMD.

$\{u_1, \ldots, u_k, \ldots, u_K\}$. For each mode, a $m \times n$ pattern matrix [40] was constructed as follows:

$$R_k = \begin{bmatrix} x_{k1} & x_{k2} & \cdots & x_{kn} \\ x_{k2} & x_{k3} & \cdots & x_{k(n+1)} \\ \vdots & \vdots & \vdots & \vdots \\ x_{km} & x_{k(m+1)} & \cdots & x_{kN} \end{bmatrix}. \tag{6}$$

The SVD was used to obtain singular values $\delta_{k1} \geq \delta_{k2} \geq \cdots \geq \delta_{kl}$ of the R_k, and the singular value spectrum of the k-th mode u_k was formulated. The singular spectrum entropy of mode u_k can be defined as follows:

$$S_k = -\sum_{i=1}^{l} q_{ki} \log q_{ki}, \tag{7}$$

where q_{ki} is the proportion of the i-th singular value in the entire singular value spectrum as follows:

$$q_{ki} = \frac{\delta_{ki}}{\sum_{j=1}^{l} \delta_{kj}}. \tag{8}$$

Applying the above method, a K-dimensional vector can be constructed from a multiscale perspective to describe the singular spectral characteristics of a signal.

2.3. Extraction of the Eigenvector. The VMD method has the ability to adaptively realize the effective separation of the frequency domain and the components of the signal, along with preserving the local characteristics of the signal, which can effectively avoid the mode-aliasing problem. In this study, based on the VMD, the singular value spectrum was obtained by the SVD of each mode, and the corresponding singular spectrum entropy was calculated. Then, the extraction of the eigenvector could be accurately realized.

The main steps of this study's signal eigenvector extraction based on the VMD method and multiscale singular spectrum entropy were as follows:

Step 1: The original signal $x = \{x_1, x_2, \ldots, x_N\}$ was decomposed using the VMD method, and the K variational mode components with different frequency bands were obtained $\{u_k\} = \{u_1, u_2, \ldots, u_K\}$.

Step 2: The m-dimensional phase space of each mode u_k was reconstructed to form the pattern matrix R_k, and the singular value spectrum $\{\delta_{k1}, \delta_{k2}, \ldots, \delta_{kl}\}$ of each mode component signal was obtained by SVD. Then, the singular spectrum entropy S_k was calculated successfully.

Step 3: The singular spectrum entropy eigenvector $T = (S_1, S_2, \ldots, S_K)$ of the original signal x was obtained by combining the singular spectrum entropy of each mode. T is used as the eigenvector to identify the rock fracture microseismic signal and the blasting vibration signal.

The feature extraction method quantificationally described the signal's frequency band information in the form of singular spectral entropy and also presented the determinations of the singular complexity of the original signal in each frequency band. The eigenvectors extracted by this method are repeatable and stable and can distinguish the two kinds of vibration signals.

2.4. Support Vector Machine. The support-vector machine (SVM) is a type of small sample learning algorithm which is based on statistical learning. It is effective in solving the problems related to small numbers of samples and nonlinear and high-dimensional pattern recognition. It has been widely applied in image recognition, fault diagnoses, etc. In this study, a least-squares support-vector machine (LS-SVM) was used to identify microseismic events. The LS-SVM is a model of the SVM which is used to solve KKT (Karush–Kuhn–Tucker) optimization problems. The LS-SVM has the ability to significantly reduce computational costs and improve the convergence speed on the basis of maintaining the standard SVM advantages [41, 42].

The basic principle is as follows:

For a given training set $Q = \{(x_i, y_i) \mid i = 1, 2, \ldots, d\}$, x_i is the i-th input data, and y_i is the output class of the i-th input data. The optimization problem of the LS-SVM can be expressed as follows:

$$\begin{aligned} &\min \quad J(w, \xi) = \frac{1}{2} w^T w + \frac{\vartheta}{2} \sum_{i=1}^{d} \xi_i^2, \\ &\text{s.t.} \quad y_i \left[w^T \Phi(x_i) + b \right] + \xi_i = 0, \quad i = 1, 2, \ldots, d, \end{aligned} \tag{9}$$

where w is the weight vector, ϑ is the adjustable constant, and b denotes the threshold value.

A Lagrange method was used to solve the optimization problem and was obtained as follows:

$$L(w, b, \xi, a) = J(w, \xi) - \sum_{i=1}^{d} a_i \left\{ y_i \left[w^T \Phi(x_i) + b \right] - 1 + \xi_i \right\}. \tag{10}$$

In the formula $a = [a_1, a_2, \ldots, a_d]$, a_i is the Lagrange multiplier, and $a_i \geq 0$. Then, by optimizing equation (10), the partial derivative could be determined as follows:

$$\begin{cases} \dfrac{\partial L}{\partial w} = 0 \Longrightarrow w = \displaystyle\sum_{i=1}^{d} a_i y_i \Phi(x_i), \\ \dfrac{\partial L}{\partial b} = 0 \Longrightarrow \displaystyle\sum_{i=1}^{d} a_i y_i = 0, \\ \dfrac{\partial L}{\partial \xi_i} = 0 \Longrightarrow a_i = \vartheta \xi_i, \\ \dfrac{\partial L}{\partial a_i} = 0 \Longrightarrow y_i \left[w^T \Phi(x_i) + b \right] - 1 + \xi_i = 0. \end{cases} \tag{11}$$

In order to avoid the problem of dimensionality caused by a direct solution, a Gauss radial basis function was introduced as the kernel function as follows:

$$K(x_i, x_j) = \exp\left(-\frac{\left\| x_i - x_j \right\|^2}{2\sigma^2} \right). \tag{12}$$

Then, after equation (12) was calculated, optimal classification equation (13) could be used to determine whether the waveform was a microseismic signal as follows:

$$f(x) = \operatorname{sgn}\left[\sum_{i,j=1}^{d} a_i K(x_i, x_j) + b \right]. \tag{13}$$

3. Proposed Identification Model

First, select an equal number of microseismic samples and blasting vibration samples, and then, perform the multiscale singular spectrum entropy calculation on the sample data and extract the eigenvector of each signal to form the training set. The LS-SVM software package is used to train the training set of the sample data to form the LS-SVM classifier. With the help of the LS-SVM classifier, the test samples can be classified. The signal identification flowchart is shown in Figure 2.

In this study, the identification algorithm of the microseismic signals based on the VMD, multiscale singular spectrum entropy, and LS-SVM (hereinafter referred to the MSSE-SVM algorithm) was as follows:

Input: the sample set Q, regularization parameter ϑ, and kernel function parameter σ^2.

Output: the classification results.

Step 1: Sample selection was done. The appropriate data were selected to form a sample set Q.

Step 2: Eigenvector extraction was done. The singular spectrum entropy eigenvector of each sample signal was extracted from the sample set Q, and the characteristics of the sample signals were represented by the multiscale singular spectrum entropy $T = (S_1, S_2, \ldots, S_K)$.

Step 3: In order to determine the LS-SVM parameters, a W-fold cross validation method was used to determine the regularization parameter ϑ and kernel function parameter σ^2. The basic process included the following: dividing the sample set Q into W parts; taking the $W-1$ parts as the training set QT; the remaining part served as the verification set QV; the classifier was trained with the QT; and the performance of the classifier was evaluated by the verification set QV. Then, the parameters were adjusted and the W times of the above process were repeated, in order to train and test all of the samples in the sample set Q. The parameters with the highest classification accuracy on the W verification set were considered to be the optimal parameters.

Step 4: Output the identification result. The trained LS-SVM classifier is used to classify the input signals and output the types of signals.

The W-fold cross validation method is the most common application and has been observed to achieve good results [43]. Finally, by taking into account the computational efficiency and references in other related research results [44], this study selected $W = 10$, $\vartheta = 1.8125$, and $\sigma^2 = 1.2075$.

The purpose of developing the MSSE-SVM algorithm is to correctly identify the microseismic signal from the microseismic detection system with high noise and blasting vibration and effectively facilitate the analysis of the microseismic signal such as source location. Compared with the similar algorithm based on EMD method, it has the merits of high noise robustness, simple operation, and suitability for small sample.

4. Experimental

4.1. Experimental Data Sources and Preprocessing. The experimental data used in this study were derived from a coal mine microseismic monitoring system located in western China, which had been mainly used for monitoring the rockburst disasters in mines. The seismic detector adopted a single component geophone sensor with a frequency response range between 3 Hz and 2 kHz. The signal sampling frequency was 1 kHz. An artificial pickup is performed to obtain a total number of 100 rock fracture microseismic signals and 100 blasting vibration signals and is recorded as the sample set Q. For the ease of analysis, data form 200 waveforms are interpreted as time sequences of equal length, and each sequence has 3000 sampling points.

4.2. Example of the Analysis Process. In this study, in order to explain the process of the feature extraction based on the VMD, singular spectrum entropy, and SVM classification, typical rock fracture microseismic and blasting vibration signals were selected from groups A and B, respectively. Then, the two signals were decomposed using the VMD method, and six variational mode components were obtained. The waveforms of the original signal, along with its variational mode components, are shown in Figure 3. The number of the sampling points N was 3000. The phase space dimension m of the pattern matrix was 300. The singular spectrum entropy of the two signals was calculated, and the results are shown in Table 1. As can be seen from Table 1, among the eigenvectors of the microseismic signal, the singular spectrum entropy of u_3 is the largest and that of u_4 is the smallest. In the eigenvectors of blasting vibration signals, the singular spectrum entropy values of u_3 and u_6 are smaller. In summary, the singular spectrum entropy could be used to characterize the singular state of the signal on the different modes.

In this study, the sample set Q was divided into two groups: A and B. In group A, there were 100 rock fracture microseismic signals observed with clear take-off waveforms, and 100 blasting vibration signals in group B. From groups A and B, 15 microseismic signals and 15 blasting vibration signals were randomly selected, respectively. Then, these signals were decomposed by VMD, and the singular spectrum entropy of each component was calculated. The results are shown in Table 2.

The average values of the singular spectrum entropy were calculated, as shown in Figure 4. It was confirmed that after the decomposition of the rock fracture microseismic signals, the singular spectrum entropy values of the two modes u_4 and u_6 were smaller, and also, mode u_3 was the maximum. In regard to the blasting vibration signals, the singular spectral entropy values of the two modes u_3 and u_6 were observed to be smaller, and the two modes u_1 and u_5 were larger. As detailed in Table 2, the singular spectrum entropy of the mode u_6 in the first five sets of blasting vibration signals was approximately 1.5. The results showed that the five sets of blasting vibration signals almost do not include vibration waves of the mode u_6, so their singular complexity is low and the singularity value is small.

From the above analysis, it was determined that the eigenvectors based on the multiscale singular spectrum entropy were stable in the same types of signals. Moreover, there were obvious differences observed in the singular spectrum entropy eigenvectors of the microseismic and blasting vibration signals, respectively. The singular spectrum entropy was found to be beneficial to the classification and identification of the two kinds of signals.

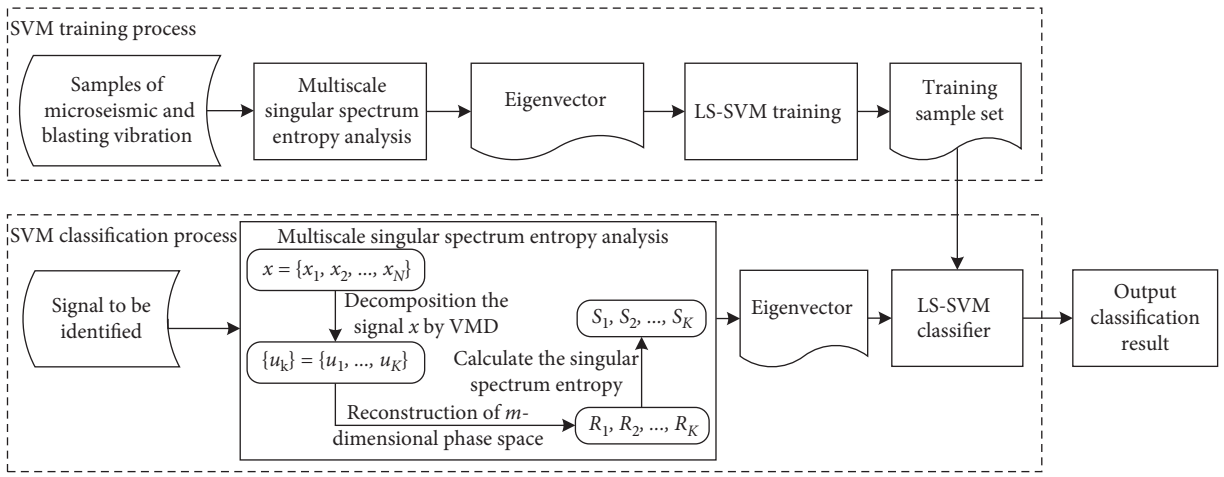

Figure 2: Signal identification flowchart.

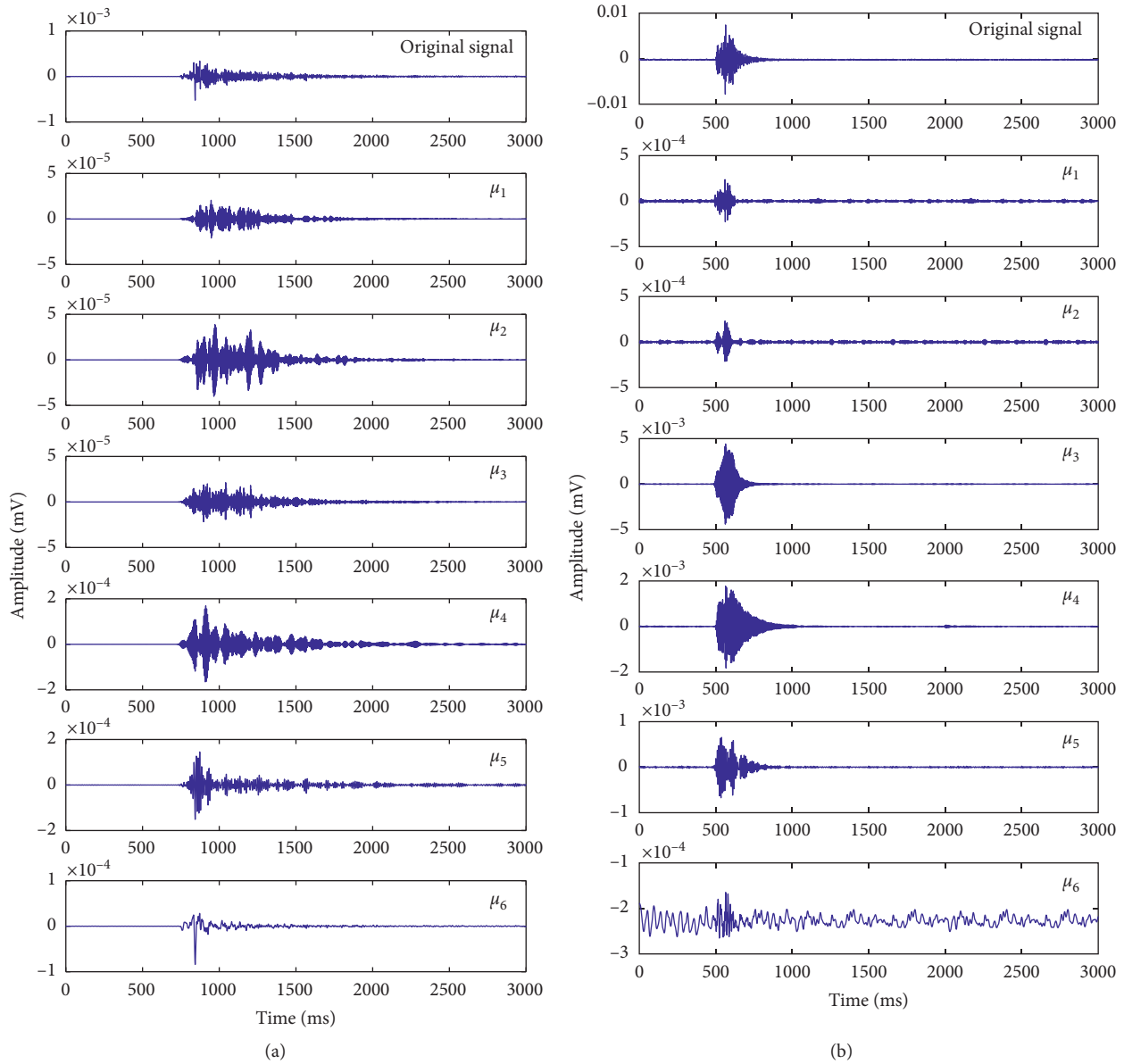

Figure 3: Original signals and VMD decomposition results. (a) The rock fracture microseismic signal. (b) The blasting vibration signal.

Table 1: Multiscale singular spectrum entropy of the two signals.

Mode no.	u_1	u_2	u_3	u_4	u_5	u_6
Microseismic signal	4.340	4.308	4.855	3.935	4.263	4.399
Blasting vibration signal	4.400	4.738	3.335	3.695	4.134	1.769

Table 2: Singular spectrum entropy of each mode of the rock fracture microseismic and blasting vibration signals.

No.	u_1	u_2	u_3	u_4	u_5	u_6
Microseismic signal						
1	4.340	4.208	4.855	3.935	4.263	4.399
2	4.377	4.361	4.715	3.738	4.369	4.001
3	4.284	4.309	4.541	4.328	4.307	3.994
4	4.301	4.442	4.919	3.923	4.141	4.005
5	4.299	4.194	4.766	3.951	4.176	4.357
6	4.237	4.231	4.743	3.771	3.893	3.528
7	4.348	4.286	4.849	3.732	4.227	4.359
8	4.226	4.240	4.734	3.763	4.433	4.125
9	4.386	4.419	4.714	4.495	4.117	4.014
10	4.164	4.104	4.576	3.501	3.889	3.717
11	4.294	4.232	4.695	3.889	3.865	3.439
12	4.206	4.178	4.743	3.685	3.962	3.529
13	4.771	4.487	4.595	3.956	4.053	3.492
14	4.284	4.213	4.781	4.598	4.318	3.834
15	4.297	4.396	4.596	4.544	4.322	3.775
Blasting vibration signal						
1	4.400	4.738	3.335	3.695	4.134	1.769
2	4.194	3.584	4.291	4.157	4.249	1.659
3	4.061	3.502	4.346	4.097	4.458	1.467
4	4.157	3.519	4.414	3.978	4.338	1.484
5	4.959	3.741	4.579	3.904	4.389	1.79
6	4.478	3.312	3.469	3.938	3.844	4.234
7	4.181	3.378	3.347	3.738	4.495	2.413
8	4.367	3.913	3.391	3.402	4.358	4.337
9	4.179	3.571	4.238	4.330	4.524	3.348
10	4.476	4.298	3.641	4.232	3.837	4.317
11	4.385	4.288	3.695	3.693	4.424	4.389
12	4.676	3.664	3.399	3.762	4.164	4.321
13	4.245	4.145	3.746	4.053	4.412	4.369
14	4.434	3.756	3.469	3.938	4.339	4.335
15	4.410	4.235	3.563	3.984	4.305	4.354

4.3. Performance of SVM Classifier and Comparative Examination. In order to test the performance of this study's algorithm, 70 groups of vibration data were selected from the groups *A* and *B*, respectively, and the training set QT was composed. The remaining 60 groups of vibration data in the two groups constituted the test set QV. The final classification results for the test set are shown in Table 3.

As can be seen from Table 3, the singular spectrum entropy could effectively characterize the features of the rock fracture microseismic signals. Among the test set QV, 30 rock microseismic signals were 100% correctly classified, and two groups of 30 blasting vibration signals were found to be misclassified, resulting in an overall classification preparation rate of 93.33%.

Then, using the 60 signals in the test set QV, a comparison between the results of this method and other methods was completed, as detailed in Table 4. It can be seen in the table that this study's method can take on higher robust and better classification comparing with the other algorithms. Although the proposed method and the energy feature method have the same classification accuracy in this test set, when we have more samples, the SVM based identification model has better adaptability and accuracy than the hard threshold method. Therefore, the proposed method was confirmed to be suitable for the classification and recognition of rock fracture microseismic signals.

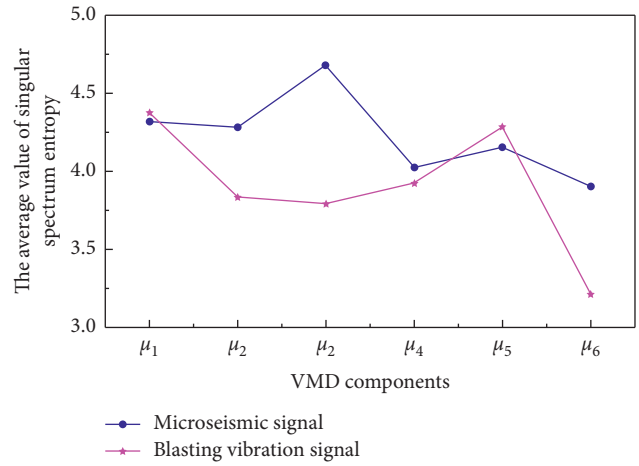

Figure 4: Multiscale singular spectrum entropy comparison chart of two kinds of signals.

5. Discussion

5.1. Influence of Singular Spectrum Entropy under Different Numbers of Sample Points. In this study, the durations of the microseismic events were relatively short, generally lasting for only approximately several seconds. When intercepting the microseismic data, the selection of the number of sampling points was determined to affect the values of the singular spectrum entropy, as well as the accuracy of the final recognition.

In order to illustrate the influences of the number of sampling points on the singular spectral entropy, a typical rock fracture microseismic signal was selected as an example (Figure 3(a)) and the number of the sample points *N* was 2,000, 3,000, 4,000, and 5,000, respectively. The time series signals of the four groups of different durations of the microseismic signals were referred to as RF1A, RF1B, RF1C, and RF1D, respectively, as shown in Figure 5.

As detailed in Figure 5, when the number of sampling points was 2,000, the tail of the microseismic event was truncated, and the microseismic waveform data were slightly deficient. However, when the number of sampling points was 3,000, 4,000, and 5,000, the microseismic waveform data were observed to be complete. The singular spectrum entropy of each of the modes of the four signals was calculated, and the results are shown in Table 5.

The singular spectrum entropy of each of the modes of the four rock fracture microseismic signals was projected to the histogram for comparison, as shown in Figure 6. In the figure, the minimum amplitudes of the two adjacent signals

Table 3: Identification results of the proposed algorithm.

Methods	Recognition accuracy (%)
30 coal rock fracture microseismic signals	100
30 blasting vibration signals	93.33

Table 4: Comparison of the three methods.

Methods	Recognition accuracy (%)
EMD + singular spectrum entropy + SVM	91.66
VMD + energy	96.66
VMD + singular spectrum entropy + SVM	96.66

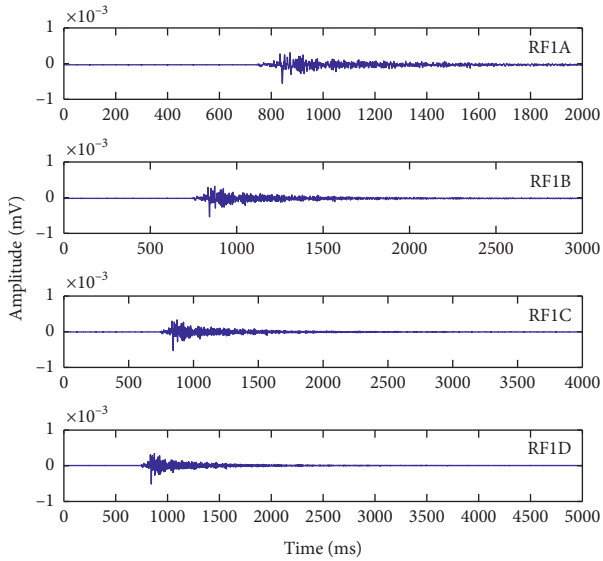

Figure 5: Different numbers of sampling points for the microseismic signals.

in the same mode on the singular spectrum entropy growth are denoted by the blue digital display, and the maximum amplitude is denoted by the red digital display. As can be seen in Figure 4, the singular spectrum entropy of each mode increased with the increases in the number of sampling points. When the number of signal sampling points changed from 3,000 to 4,000, the maximum increased amplitude difference of the singular spectrum entropy of each mode was 0.1, and the singular spectrum entropy of the modes maintained the same increase difference. When the number of signal sampling points changed from 4,000 to 5,000, the maximum increased amplitude difference of the singular spectrum entropy of each mode was 0.07, and the singular spectrum entropy of the modes also maintained the same increase difference. However, when the number of signal sampling points changed from 2,000 to 3,000, the maximum increase in the amplitude difference of the singular spectrum entropy of each mode was 0.513, and the singular spectrum entropy increases between the modes were observed to be quite different.

Table 5: Singular spectrum entropy of each of the modes of the four signals.

N	u_1	u_2	u_3	u_4	u_5	u_6
2000	3.953	3.820	4.275	3.429	3.586	3.499
3000	4.340	4.308	4.855	3.935	4.263	4.399
4000	4.608	4.577	5.128	4.207	4.538	4.677
5000	4.818	4.786	5.341	4.419	4.752	4.893

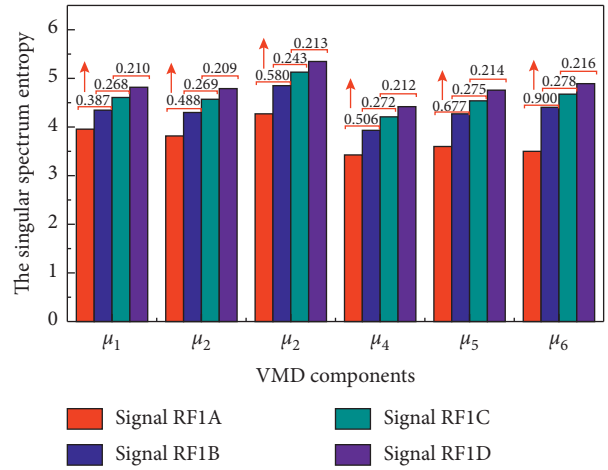

Figure 6: Singular spectrum entropy histogram of the four signals.

In this study, following the training of the LS-SVM classifier, it is usually necessary to normalize each component value of an eigenvector to a [0, 1] interval in order to form a standardized eigenvector. The purpose was to speed up the training speed and improve the classification accuracy. The normalized eigenvectors of the four singular spectral entropy feature vectors detailed in Table 4 are shown in Figure 7. As can be seen in Figure 7, the RF1A was very different from the singular spectrum entropy standard eigenvectors of the other three microseismic signals. However, the singular spectrum entropy standard eigenvectors of RF1B, RF1C, and RF1D were found to be almost the same. It was found that when the number of sampling points was 2,000, the data of RF1A were deficient, and the eigenvector lacked reliability. However, when the number of sampling points was 3,000, 4,000, and 5,000, the data of RF1B, RF1C, and RF1D were observed to be complete, and the eigenvectors were determined to be reliable. Therefore, it was necessary to pay attention to the influences of the number of sampling points on the eigenvectors of the singular spectrum entropy. In accordance with the results of the large number of experiments completed in this study, it was suggested that 3,000 sampling points were more suitable for both the rock fracture microseismic signals and the blasting vibration signals.

5.2. Investigation of Identification Result under Different K Values. From the previous discussion, it can be seen that each signal could be used as a six-dimensional singular spectrum entropy vector to express its characteristics. In order to reveal the effect of the K value on identification

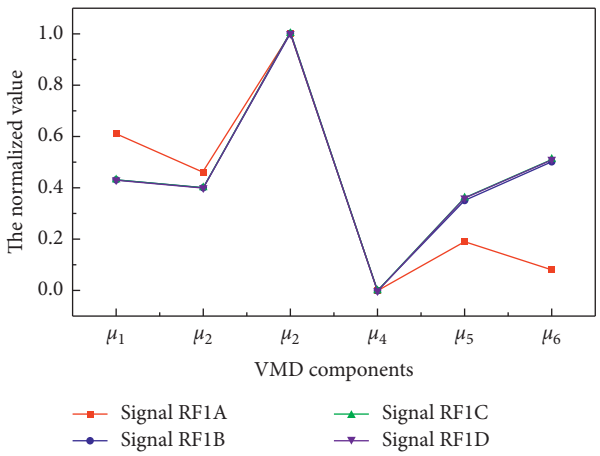

Figure 7: Normalized singular spectrum entropy of the four signals.

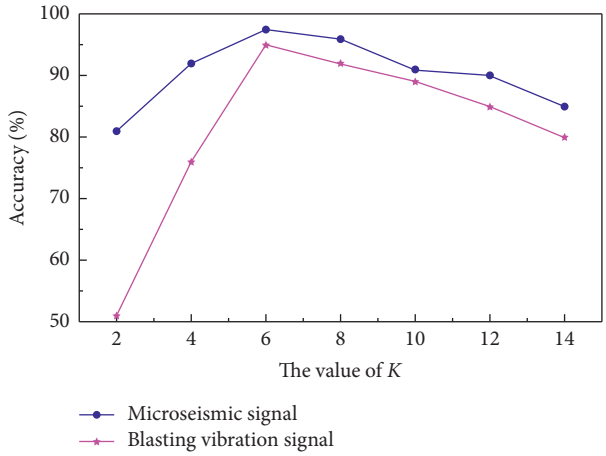

Figure 8: Influences of the K values on the identification accuracy.

results, 100 rock fracture microseismic signals and 100 blasting vibration signals were used in this study, of which K was 2, 4, 6, 8, 10, 12, and 14, respectively. The identification accuracy at the different K values is shown in Figure 8.

It is clear in Figure 8 that when the K value was 2, the identification accuracy of the blasting vibration signal was approximately 50%, and the identification accuracy of the rock fracture microseismic signal was approximately 80%. As the K values increased, the identification accuracy was also observed to increase. This was found to be due to the increased K values causing the layer of signal decomposition to increase, allowing for a more accurate expression of the complexity of the signal. Therefore, the differences in the rock fracture microseismic and blasting vibration signals were more easily distinguished. However, when the K value was more than 6, the accuracy rate of the identification was observed to be reduced. These results were due to the fact that when the number of the modes was too high, over decomposition of the signal occurred. When the original signal had only a very small number of signals in some of the modes, the singular spectrum entropy of the mode may have been too high or too low, and the differences in the singular spectral entropy eigenvectors of the two kinds of signals were observed to be affected. In accordance with the results of the experiments conducted in this study, it was suggested that the K value was 6.

6. Conclusions

In this paper, the identification model of the microseismic signal is established to accurately identify and record the microseismic signal under the influence of blasting vibration signals. The microseismic signal identification method is proposed with a combination of MSSE and SVM based on the LS-SVM theory, which can effectively distinguish the microseismic signal and blasting vibration signal and has high identification accuracy and stability. We can draw the following conclusions form the results of numerical computation and experiment:

(1) Compared with EMD and wavelet analysis, the VMD algorithm captures the relevant center frequencies quite precisely, the resulting signal separation is relatively good, and the frequency of each mode is more compact and clear. The main problem of the application of the VMD algorithm is to determine the value of K, which is related to the signal-to-noise ratio and dominant spectrum distribution of the signal.

(2) The number of sampling points of the signals have certain influences on the eigenvector of the singular spectral entropy. It was determined that when the number of sampling points was 3000, the singular spectral entropy eigenvectors of the same types of vibration signals could reach a stable state.

(3) The model experiment demonstrated that the multiresolution singular spectrum entropy can be used as a classification feature to classify and identify the rock fracture microseismic and blasting vibration signals. It was verified that the proposed method has high identification accuracy.

Data Availability

All data included in this study are available upon request by contact with the corresponding author.

Conflicts of Interest

The authors declare that they have no conflicts of interest regarding the publication of this paper.

Acknowledgments

This work was funded by the National Key Research and Development Program of China (no. 2017YFC0804406), National Natural Science Foundation of China (no. 51904173), Shandong Provincial Natural Science Foundation (no. ZR2018MEE008), and Project of Shandong Province Higher Educational Science and Technology Program (no. J18KA307).

References

[1] R. Allen, "Automatic earthquake recognition and timing from single traces," *Bulletin of the Seismological Society of Americ*, vol. 68, no. 5, pp. 1521–1532, 1978.

[2] R. Allen, "Automatic phase pickers: their present use and future prospects," *Bulletin of the Seismological Society of America*, vol. 72, no. 6B, pp. S225–S242, 1982.

[3] M. Baer and U. Kradolfer, "An Automatic phase picker for local and teleseismic events," *Bulletin of the Seismological Society of America*, vol. 77, no. 4, pp. 1437–1445, 1987.

[4] H. Akaike, "Information theory and an extension of the maximum likelihood principle," in *Proceedings of the 2nd International Symposium on Information Theory*, pp. 267–281, Akademiai Kaido, Budapest, Hungary, 1973.

[5] C.-P. Lu, L.-M. Dou, X.-R. Wu, H.-M. Wang, and Y.-H. Qin, "Frequency spectrum analysis on microseismic monitoring and signal differentiation of rock material," *Chinese Journal of Geotechnical Engineering*, vol. 27, no. 7, pp. 772–775, 2005.

[6] P.-F. Alvanitopoulos, M. Papavasileiou, I. Andreadis, and A. Elenas, "Seismic intensity feature construction based on the Hilbert-Huang transform," *IEEE Transactions on Instrumentation and Measurement*, vol. 61, no. 2, pp. 326–337, 2012.

[7] S. Gaci, "The use of wavelet-based denoising techniques to enhance the first-arrival picking on seismic traces," *IEEE Transactions on Geoscience and Remote Sensing*, vol. 52, no. 8, pp. 4558–4563, 2014.

[8] S. Tang, M. Tong, Y. Pan, X. He, and X. Lai, "Energy spectrum coefficient analysis of wavelet features for coal rupture microseismic signal," *Chinese Journal of Scientific Instrument*, vol. 32, no. 7, pp. 1522–1527, 2011.

[9] Q. J. Zhu, F. Jiang, Z. Yu, Y. Yin, and L. Lu, "Study on energy distribution characters about blasting vibration and rock fracture microseismic signal," *Chinese Journal of Rock Mechanics and Engineering*, vol. 31, no. 4, pp. 723–730, 2012.

[10] F.-X. Jiang, Y.-M. Yin, Q. J. Zhu, S.-X. Li, and Z.-X. Yu, "Feature extraction and classification of mining microseismic waveforms via multi-channels analysis," *Journal of the China Coal Society*, vol. 39, no. 2, pp. 229–237, 2014.

[11] S. Saha, D. Mukherjee, and S. Mukhopadhyay, "Online detection and location estimation of earthquake events using continuous wavelet transform," in *Proceedings of the 2016 IEEE First International Conference on Control, Measurement and Instrumentation (CMI)*, Kolkata, India, January 2016.

[12] N. Karamzadeh, G. J. Doloei, and A. M. Reza, "Automatic earthquake signal onset picking based on the continuous wavelet transform," *IEEE Transactions on Geoscience and Remote Sensing*, vol. 51, no. 5, pp. 2666–2674, 2013.

[13] P. Han, K. Hattori, Q. Huang et al., "Evaluation of ULF electromagnetic phenomena associated with the 2000 Izu Islands earthquake swarm by wavelet transform analysis," *Natural Hazards and Earth System Science*, vol. 11, no. 3, pp. 965–970, 2011.

[14] Q. J. Zhu, F.-X. Jiang, Y.-M. Yin, Z.-X. Yu, and J.-L. Wen, "Classification of mine microseismic events based on wavelet-fractal method and pattern recognition," *Chinese Journal of Geotechnical Engineering*, vol. 34, no. 11, pp. 2036–2042, 2012.

[15] N. E. Huang, Z. Shen, S. R. Long et al., "The empirical mode decomposition and Hilbert spectrum for nonlinear and non-stationary time series analysis," *Proceedings of the Royal Society A Mathematical Physical & Engineering Sciences*, vol. 454, no. 1971, pp. 903–995, 1998.

[16] R.-S. Jia, Y.-Q. Liang, Y.-C. Hua, H.-M. Sun, and F.-F. Xia, "Suppressing non-stationary random noise in microseismic data by using ensemble empirical mode decomposition and permutation entropy," *Journal of Applied Geophysics*, vol. 133, pp. 132–140, 2016.

[17] X. Wu, J. Qian, H. Wang, and H. Qin, "Study on multi-scale nonlinear feature extraction and signal identification for microseismic signal," *Chinese Journal of Scientific Instrument*, vol. 35, no. 5, pp. 969–975, 2014.

[18] X. Y. Shang, X.-B. Li, K. Peng, L. J. Dong, and Z. W. Wang, "Feature extraction and classification of mine microseism and blast based on EMD-SVD," *Chinese Journal of Geotechnical Engineering*, vol. 38, no. 10, pp. 1849–1858, 2016.

[19] R.-S. Jia, H.-M. Sun, Y.-J. Peng, Y.-Q. Liang, and X.-M. Lu, "Automatic event detection in low SNR microseismic signals based on multi-scale permutation entropy and a support vector machine," *Journal of Seismology*, vol. 21, no. 4, pp. 1–14, 2017.

[20] L. J. Dong, J. Wesseloo, Y. Potvin, and X. Li, "Discrimination of mine seismic events and blasts using the fisher classifier, Naive Bayesian classifier and logistic regression," *Rock Mechanics and Rock Engineering*, vol. 49, no. 1, pp. 183–211, 2016.

[21] X. L. Zhang, X. M. Lu, R. S. Jia, and S. T. Kan, "Micro-seismic signal denoising method based on variational mode decomposition and energy entropy," *Journal of China Coal Society*, vol. 43, no. 2, pp. 356–363, 2018.

[22] H. M. Zhao, J. J. Zheng, W. Deng, and Y. J. Song, "Semi-supervised broad learning system based on manifold regularization and broad network," *IEEE Transactions on Circuits and Systems I: Regular Papers*, vol. 67, no. 3, pp. 983–994, 2020.

[23] W. Deng, J. J. Xu, and H. M. Zhao, "An improved ant colony optimization algorithm based on hybrid strategies for scheduling problem," *IEEE Access*, vol. 7, pp. 20281–20292, 2019.

[24] G.-y. Zhao, J. Ma, L.-j. Dong, X.-b. Li, G.-h. Chen, and C.-x. Zhang, "Classification of mine blasts and microseismic events using starting-up features in seismograms," *Transactions of Nonferrous Metals Society of China*, vol. 25, no. 10, pp. 3410–3420, 2015.

[25] J. Ma, G. Y. Zhao, L. J. Dong, G. H. Chen, and C. X. Zhang, "A comparison of mine seismic discriminators based on features of source parameters to waveform characteristics," *Shock and Vibration*, vol. 2015, Article ID 919143, 10 pages, 2015.

[26] B. L. Li, N. Li, E. Y. Wang, X. L. Li, X. Zhang, and Y. Niu, "Discriminant model of coal mining microseismic and blasting signals based on waveform characteristics," *Shock and Vibration*, vol. 2017, Article ID 6059239, 13 pages, 2017.

[27] K. Dragomiretskiy and D. Zosso, "Variation mode decomposition," *IEEE Transactions on Signal Processing*, vol. 62, no. 3, pp. 531–544, 2014.

[28] P. Xie, F.-M. Yang, X.-X. Li, Y. Yang, X. L. Chen, and L.-T. Zhang, "Functional coupling analyses of electroencephalogram and electromyogram based on variational mode decomposition-transfer entropy," *Acta Physica Sinica*, vol. 65, no. 11, pp. 11870-11871, 2016.

[29] G. J. Tang and X. L. Wang, "Parameter optimized variational mode decomposition method with application to incipient fault diagnosis of rolling bearing," *Journal of Xi'an Jiaotong University*, vol. 49, no. 5, pp. 73–81, 2015.

[30] M. Zhang, Y. L. Zhu, N. Zhang, and Y. Y. Zhang, "Feature extraction of transformer partial discharge signals based on varitional mode decomposition and multi-scale permutation entropy," *Journal of North China Electric Power University*, vol. 43, no. 6, pp. 31–37, 2016.

[31] X.-L. Zhang, R.-S. Jia, X.-M. Lu, Y.-J. Peng, and W.-D. Zhao, "Identification of blasting vibration and coal-rock fracturing microseismic signals," *Applied Geophysics*, vol. 15, no. 2, pp. 280–289, 2018.

[32] Y. Zhu, X. Shi, and P. Li, "Classification of islanding and grid disturbance based on multi-resolution singular spectrum entropy and SVM," *Proceedings of the CSEE*, vol. 31, no. 7, pp. 64–70, 2011.

[33] H. Li, M. Jiao, X. Yang, L. Bai, and X. Luo, "Fault diagnoisis of hydroelectric sets based on EEMD and SOM neural networks," *Journal of Hydroelectric Engineering*, vol. 36, no. 7, pp. 83–91, 2017.

[34] J. Wang, R. Jia, and B. Tan, "Fault diagnosis of wind turbine's gearbox based on eemd and fuzzy C means clustering," *Acta Energiae Solaris Sinica*, vol. 36, no. 2, pp. 319–324, 2015.

[35] M. Ahmadipour, H. Hizam, M. L. Othman, M. A. M. Radzi, and N. Chireh, "A fast fault identification in a grid-connected photovoltaic system using wavelet multi-resolution singular spectrum entropy and support vector machine," *Energies*, vol. 12, no. 13, p. 2508, 2019.

[36] V. N. Vapnik, "An overview of statistical learning theory," *IEEE Transactions on Neural Networks*, vol. 10, no. 5, pp. 988–999, 1999.

[37] A. Widodo and B.-S. Yang, "Support vector machine in machine condition monitoring and fault diagnosis," *Mechanical Systems and Signal Processing*, vol. 21, no. 6, pp. 2560–2574, 2007.

[38] Y.-C. Wu, Y.-S. Lee, and J.-C. Yang, "Robust and efficient multiclass SVM models for phrase pattern recognition," *Pattern Recognition*, vol. 41, no. 9, pp. 2874–2889, 2008.

[39] J. A. K. Suykens and J. Vandewalle, "Least squares support vector machine classifiers," *Neural Processing Letters*, vol. 9, no. 3, pp. 293–300, 1999.

[40] H. M. Zhao, H. D. Liu, J. J. Xu, and W. Deng, "Performance prediction using high-order differential mathematical morphology gradient spectrum entropy and extreme learning machine," *IEEE Transactions on Instrumentation and Measurement*, vol. 99, p. 1, 2019.

[41] A. Chamkalani, "Application of LS-SVM classifier to determine stability state of asphaltene in oilfields by utilizing SARA fractions," *Petroleum Science and Technology*, vol. 33, no. 1, pp. 31–38, 2015.

[42] J. S. Mary, M. A. S. Balaji, A. Krishnakumari, R. S. Nakandhrakumar, and D. Dinakaran, "Monitoring of drill runout using least square support vector machine classifier," *Measurement*, vol. 146, pp. 24–34, 2019.

[43] J. G. Moreno-Torres, J. A. Saez, and F. Herrera, "Study on the impact of partition-induced dataset shift on *k*-fold cross-validation," *IEEE Transactions on Neural Networks and Learning Systems*, vol. 23, no. 8, pp. 1304–1312, 2012.

[44] H. Ling, C. Qian, W. Kang, C. Liang, and H. Chen, "Combination of support vector machine and *K*-fold cross validation to predict compressive strength of concrete in marine environment," *Construction and Building Materials*, vol. 206, pp. 355–363, 2019.